

Preparation, morphology and surface functionalization of electrospun polyamide 6 composite nanofibers

Yibing Cai¹, Xin Xia^{1,2}, Qufu Wei^{1*}, Fenglin Huang¹, Aiwei Wang¹, Weidong Gao¹

1. Key Laboratory of Eco-Textiles, Ministry of Education, Jiangnan University, Wuxi 214122, Jiangsu, People's Republic of China

2. Xinjiang University, Wulumuqi, 830046, Xinjiang, People's Republic of China

Corresponding to: Qufu Wei (qfwei@jiangnan.edu.cn)

Abstract

In the present work, the polyamide6 (PA6) nanofiber and PA6/organophilic montmorillonites (OMT) composite nanofiber were firstly prepared by a facile compounding process with electrospinning, and then coated by nano-Fe₂O₃ using magnetron sputter technique. The structure, surface morphology and thermal stability properties were characterized by X-ray diffraction (XRD), Scanning electron microscope (SEM), Energy dispersive X-ray spectroscopy (EDX), Atomic force microscope (AFM) and Thermogravimetric analyses (TGA), respectively. It was found that the OMT layers were well dispersed within the composite nanofiber. The SEM images showed that the diameters of composite nanofiber were decreased comparing to the PA6 nanofiber, and the nano-Fe₂O₃ well coated on the surface of homogeneous and cylindrical nanofiber. The EDX confirmed the presences of the OMT and nano-Fe₂O₃ in the fibers. The AFM images showed that there was a remarkable difference in the surface morphology of composite nanofiber before and after sputter coating. The TGA analysis indicated the barrier effects of silicate clay layers and catalysis effects of nano-Fe₂O₃ improved thermal stability properties of the composite nanofiber.

Supported by the Research Fund for the Doctoral Program of Higher Education of China (No. 200802951011), the Natural Science Initial Research Fund of Jiangnan University (No. 2008LYY002) and the Program for New Century Excellent Talents in University (No. NCET-06-0485).

Keywords: electrospinning, PA6/OMT composite nanofibers, sputter coating, surface morphology, thermal stability

1 Introduction

Polymer/clay nanocomposites (PCN) have attracted much attention from researchers in the last decade owing to their increased modulus and strength and improved thermal and barrier properties[1-2]. The dispersion of these ultrathin (1nm) ultrahigh-surface-area clay layers (usually lower than 5%) within a polymer matrix leads to PCN exhibiting remarkably improved physicochemical properties, better dimensional and thermal stabilities, improved gas barrier properties, and reduced flammability compared with pure polymers or conventional microcomposites[3-4]. Electrospinning provided not only a homogeneous dispersion within the fibers of MMT, but also yielded a drastic decrease in the fiber diameter down to several tens of nanometers. It was reported that the structure, morphology, crystalline properties of PA6/clay nanocomposite fibers by electrospinning[5-7]. In addition, the mechanical property of electrospun PA6/clay nanofibers was investigated using AFM[7]. However, there are a few reports on the thermal stability and flammability properties of composite nanofibres[8].

Another emerging nanoparticles which have also shown promising effects on polymer thermal degradation are metal oxides particles, such as Al_2O_3 , TiO_2 , Fe_2O_3 . The use of oxide particles in the submicronic or nanometric range as synergistic agents in addition to usual fire retardant additives seems to be very promising. It has been also noticed that their nanometric size made them suitable for synergistic effects with organoclays, allowing fire behavior performances to be improved [9-11].

In the present work, the PA6 nanofiber and PA6/OMT composite nanofiber were firstly prepared by a facile compounding process with electrospinning, and then coated by nano- Fe_2O_3 using magnetron sputter technique. The sputtering technology has been widely used to deposit very thin films on various substrates for commercial and scientific purposes. The ability to deposit well-controlled coatings on nanofibers would expand the application of nanofibers, based on changes to both the physical and

chemical properties of the nanofibers. The structure, surface morphology and thermal stability properties were respectively characterized by XRD, SEM, EDX, AFM and TGA.

2 Experimental

2.1 Materials

The organophilic montmorillonites (OMT) by hexadecyl trimethyl ammonium bromide (cation exchange capacity, CEC, 97meq/100g of clay) was purchased from Zhejiang Fenghong Clay Chemicals Co., Ltd. Polyamide6 (PA6, 1003NW8, with weight-average molecular weight 18000) was supplied as pellets by UBE Industries, Japan. 99.5% N, N-dimethyl formamide (DMF) and 88% formic acid were all used as received.

2.2 Preparation of PA6 composite nanofibers

The slurry was prepared by dispersing OMT (2g) powder into DMF (24.26ml) solvent using magnetic stirring for 30min until the powder uniformly dispersed in the DMF solvent, and then sonicated for 1.5h. 15 wt% of PA6 dissolved in formic acid was also prepared. The prepared clay slurry was then put into the PA6 solution, which was mixed by magnetic stirring for 30min and then was sonicated for another 20min. The polymer solutions were electrospun at a positive voltage of 14 kV with a working distance of 10cm (the distance between the needle tip and the collection plate), and an ejection rate of 0.2ml/h. The mass ratio of the OMT to PA6 was 4wt% and was referred to as PA6/OMT composite nanofiber.

2.3 Sputter coating

The magnetron sputter coating system JZCK-420B (Shenyang, Juzhi Co., Ltd.) was used to deposit a nanolayer on the composite nanofibers. A high purity Fe₂O₃ target (99.999%) was mounted on the cathode, and the nanofibers substrate was placed on the anode with a side facing the target. Argon pressure was set at 0.5Pa. The Radio Frequency (RF) power used for Fe₂O₃ sputtering was set at 120W. The thickness of the

deposition layer was 100nm, which was measured using Inficon XTM in situ film thickness monitor.

2.4 Characterization

2.4.1 XRD analysis

X-ray diffraction (XRD) patterns were performed on the 1 mm thick films using a Japan Rigaku D/Max-Ra rotating-anode X-ray diffractometer equipped with a CuK α tube and Ni filter ($\lambda = 0.1542$ nm).

2.4.2 SEM and EDX analyses

Scanning electron microscope (SEM) Quanta 200 was used to examine the structures of the composite nanofibers. The samples were coated with a thin layer of gold by sputtering before the SEM imaging. The SEM Quanta 200 equipped with Energy dispersive X-ray spectroscopy (EDX) was used to examine the chemical compositions of the sputter coated nanofibers. An accelerating voltage of 20kV with accounting time of 100s was applied.

2.4.3 Surface morphology

The atomic force microscope (AFM) was used to further observe the surface structures of the composite nanofibers. The AFM used in this work was a Benyuan CSPM 4000. Scanning was carried out in tapping mode. All images were obtained at ambient conditions.

2.4.4 Thermal stability properties

Thermogravimetric analyses (TGA) were carried out using a TGA50H thermo-analyzer instrument from 25 to 700°C using a linear heating rate of 10°C/min under nitrogen flow. The nitrogen flow was 25ml/min. Samples were measured in a sealed alumina pan with a mass of about 10mg.

3 Results and discussion

3.1 Structure and morphology

Figure 1 shows the XRD patterns of the OMT and PA6/OMT composite nanofibers. The maximum peaks corresponded to the (001) plane reflection of the clays. The d_{001} peak of the OMT at $2\theta = 3.7^\circ$ corresponded to a 2.39 nm interlayer spacing. Meanwhile, the diffraction peak at $2\theta = 7.4^\circ$ in Figure 1 corresponded to the (002) plane reflection of the OMT, and the interlayer spacing was round 1.70 nm. There were no observable diffraction peaks for PA6/OMT composite nanofibers, as indicated in Figure 1. This means that most of the MMT was exfoliated and well dispersed in the PA6 composite nanofibers.

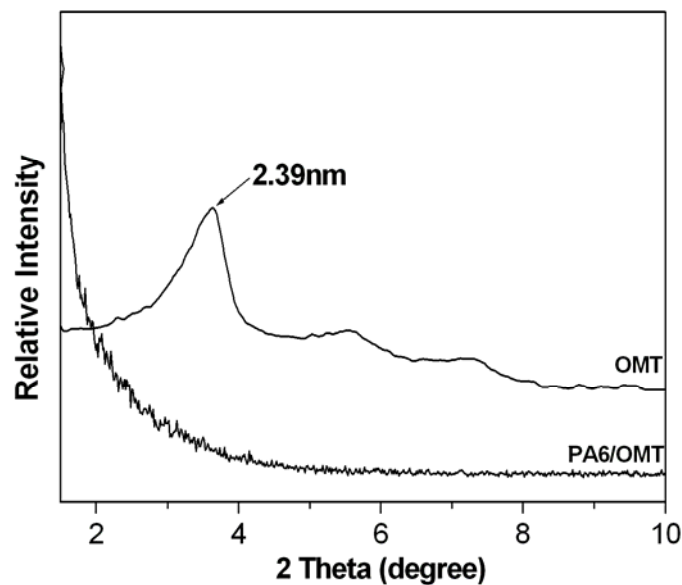


Figure 1. XRD patterns of the OMT, and PA6/O-MMT composite nanofibres.

The SEM images of electrospun PA6 nanofiber and PA6/OMT composite nanofibers, collected on the aluminum foil, are illustrated in Figure 2. The nanofibers were randomly distributed to form the three-dimensional fibrous web. It was clearly observed the formation of beaded structures of the nanofibers, contributed to the aggregation of the OMT, as indicated in Figure 2(b). Meanwhile, it was found that the electrospun nanofibers with variable fiber diameters. Compared to the PA6 nanofibers (Figure 2(a)), the average diameters of the PA6/OMT composite nanofibers (Figure 2(b)) were decreased with OMT loading. This was because the loading of OMT

contained a quaternary ammonium ion ($C_{16}H_{33}(CH_3)_3N^+$) as an organic modifier, and Na^+ and Ca^{2+} ions located between clay layers increased the charge density and conductivity of the PA6 solution[12-13], leading to the decrease in the average diameter of the PA6/OMT composite nanofiber.

The morphology of PA6 nanofiber and PA6/OMT composite nanofibers after sputter coating was also shown in Figure 3. It was observed that the ellipsoidal-like Fe_2O_3 nanoparticles were well deposited on the surface of nanofibers.

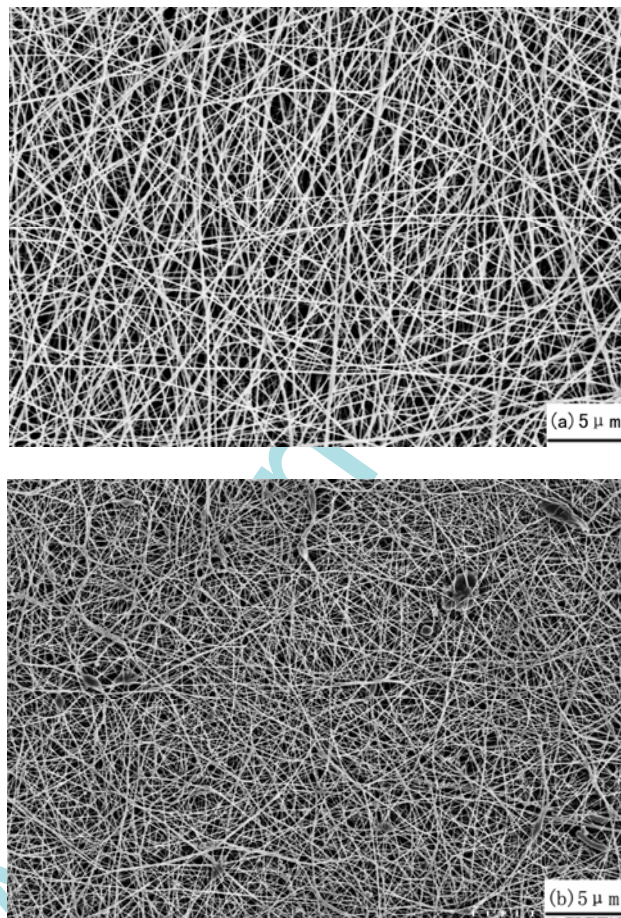


Figure 2. SEM images of (a) PA6 nanofiber and (b) PA6/OMT composite nanofiber.

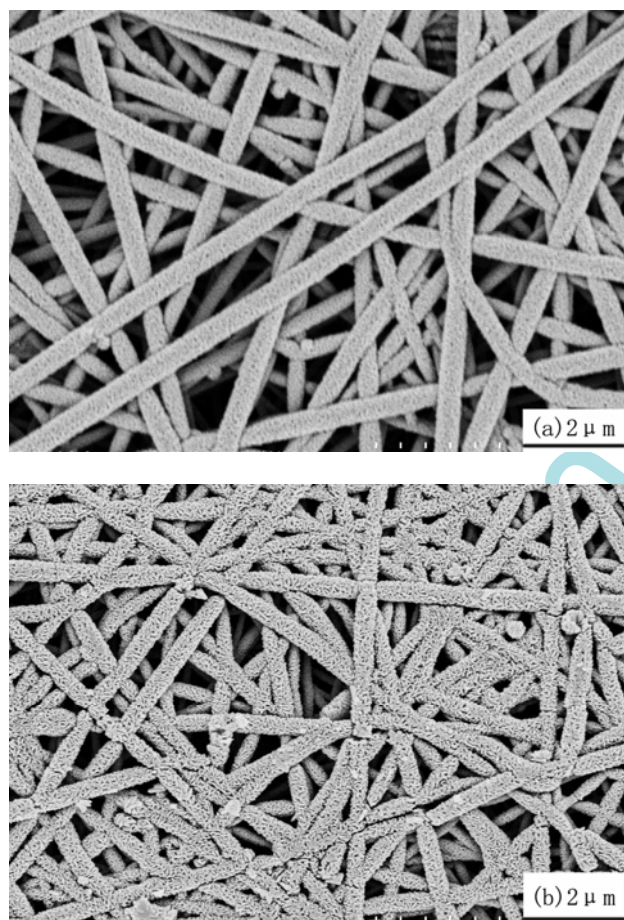
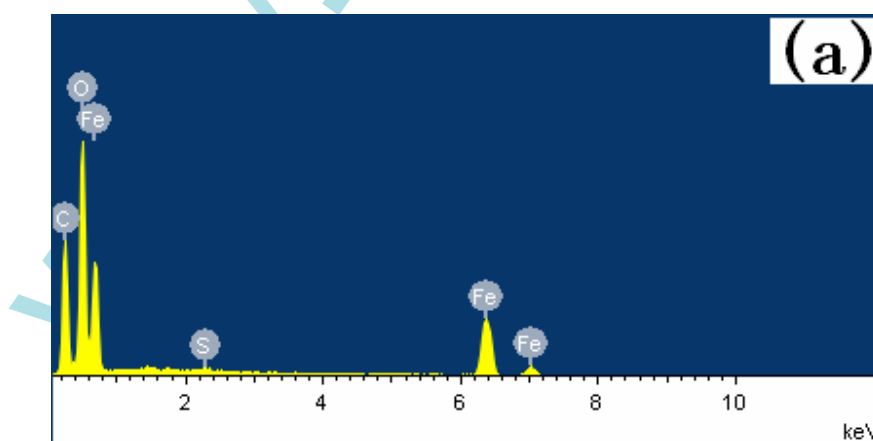


Figure 3. SEM images of (a) coated PA6 nanofiber and (b) coated PA6/OMT composite nanofiber.

3.2 EDX analysis



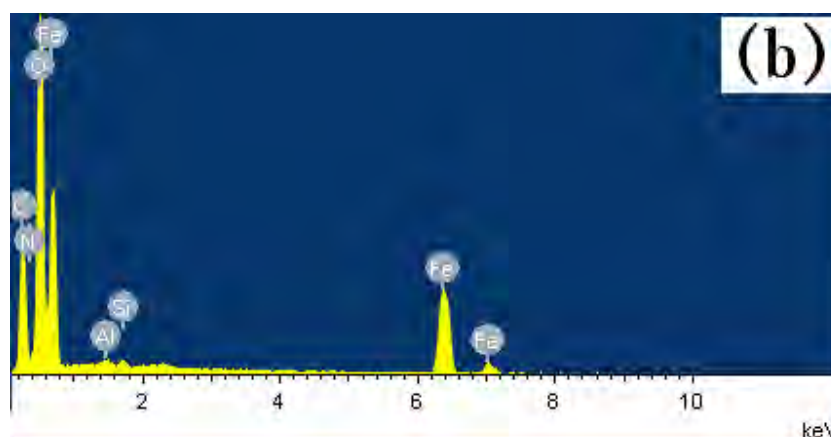


Figure 4. EDX spectra of (a) coated PA6 nanofiber and (b) coated PA6/OMT composite nanofiber.

Figure 4 shows the EDX spectra of the coated PA6 nanofiber and coated PA6/OMT composite nanofiber. It can be seen that the coated fibers dominantly consisted of C, O and Fe, deriving from the PA6 and the surface coated Fe_2O_3 nanoparticles, respectively. It can be also be found that the amount of O became higher (Figure 4(b)) compared with that in Figure 4(a), due to the contributions of OMT. The significant amount of Al and Si within the PA6/OMT composite nanofiber can also be seen in Figure 4(b), attributed to the OMT within the nanofiber.

3.3 Surface morphology

The surface morphology of electrospun fibers after sputter coating was investigated using AFM, as indicated in Figure 5. Sputter coating significantly altered the surface characteristics of the nanofibers. It can be seen that the Fe_2O_3 nanoparticles were quite uniformly distributed on surface of the nanofiber. And the Fe_2O_3 nanoparticles with variable sizes formed the rougher surface. The AFM image also revealed that the coated Fe_2O_3 nanoparticles for the PA6/OMT composite nanofibers (Figure 5(b)) looked more compact than those on the PA6 nanofibers (Figure 5(a)). The reasons may be that the loading of OMT reduced the interface tensions between the nanofibers and the nano- Fe_2O_3 , and was propitious to the depositions of Fe_2O_3 nanoparticles. The smoothness of the Fe_2O_3 film was improved and the sputtered film became more compact.

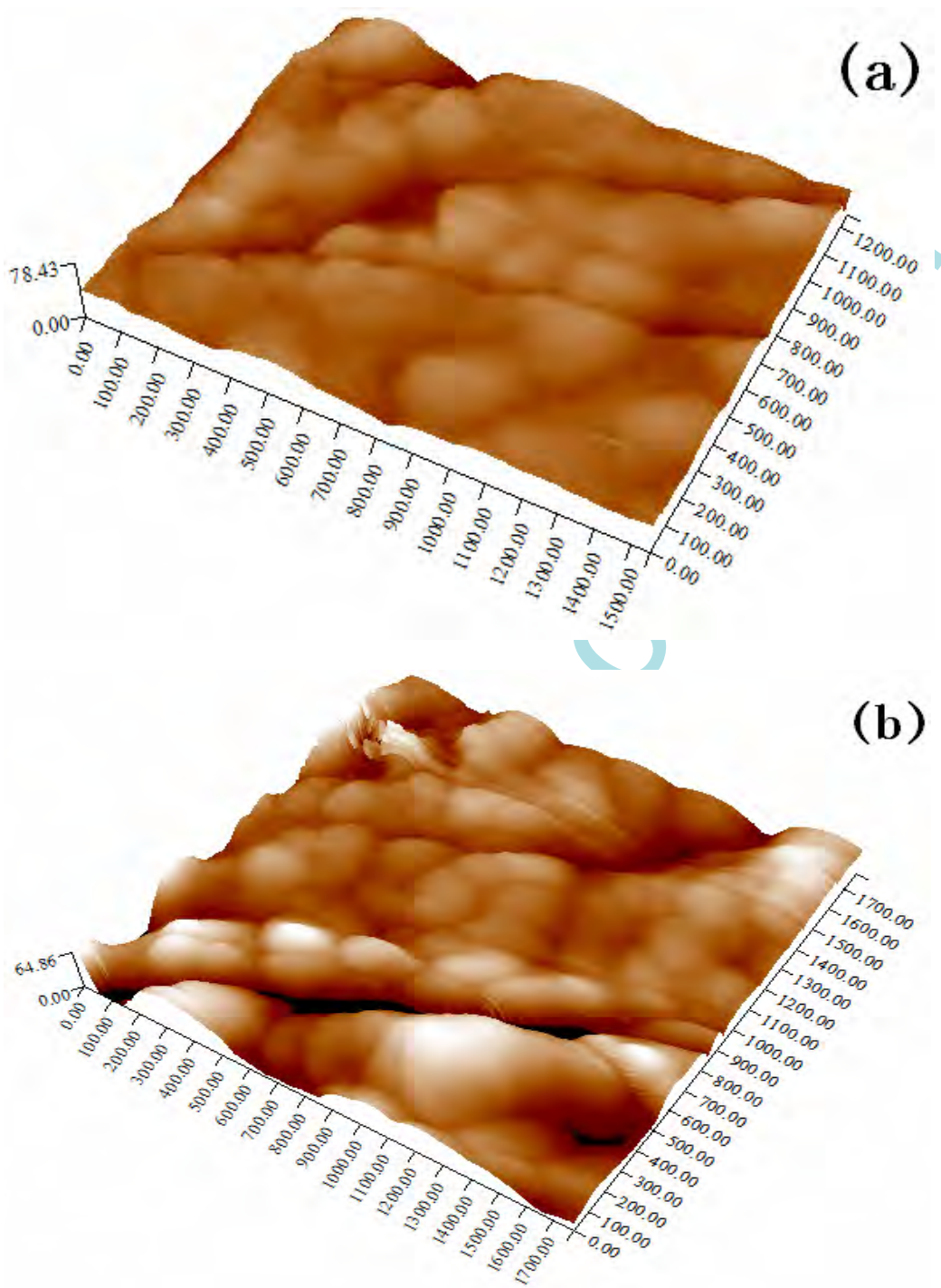


Figure 5. AFM images of the (a) coated PA6 nanofiber and (b) coated PA6/OMT composite nanofiber.

3.4 Thermal stability properties

The TGA curves for PA6 nanofiber, PA6/OMT composite nanofiber and coated PA6/OMT composite nanofiber are shown in Figure 6. The onset thermal stability of PA6/OMT composite nanofiber and coated PA6/OMT composite nanofiber showed a slight decrease, compared to the PA6 nanofibers. The reasons for this may be that the alkylammonium cations were thermally unstable and degraded in advance. Meanwhile, the catalysis effects of some transition metals cations (e.g., Fe^{3+}) may decrease the thermal stability of PA6 nanofiber[14]. It was also suggested that Fe^{3+} cations facilitated decomposition of hydroperoxides through a reversible oxidative- reductive catalytic process between Fe^{3+} and Fe^{2+} [15].

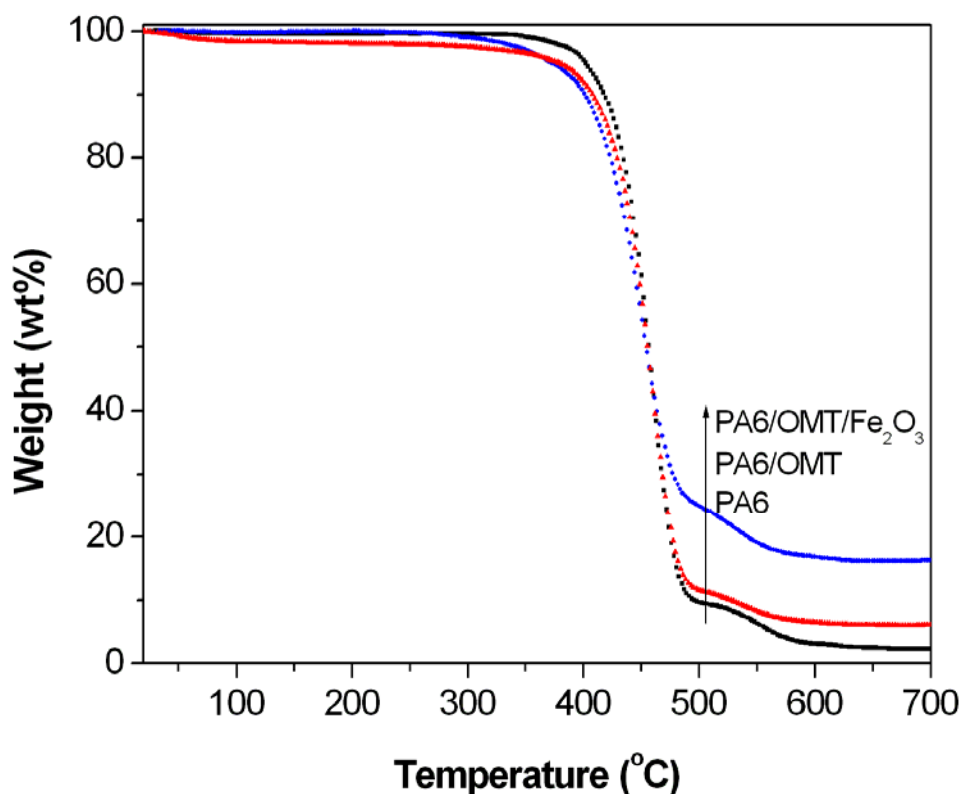


Figure 6. TGA curves of the PA6 nanofiber, PA6/OMT composite nanofiber and coated PA6/OMT composite nanofiber.

However, the yield of charred residue at 700°C for the PA6/OMT composite nanofibers before and after sputter coating were higher than that of the PA6 nanofiber.

This was attributed to the silicate clay layers which could presumably facilitate the reassembly of lamellae to form three-dimensional char, which might occur on the surface of the composite nanofibers and create a physical protective barrier. The silicate clay layers could also act as a superior insulator and mass-transport barrier and subsequently mitigate the escape of volatile products generated during the thermal decomposition[3,16]. Meanwhile, the Fe ion was the operative site for radical trapping and increased charring processes coated PA6/OMT composite nanofibers[17]. The increased charred residue contributed to the improved thermal stability of composite nanofibers.

4 Conclusions

The PA6/OMT composite nanofibers were prepared by a facile compounding and electrospinning. The surface functionalization of composite nanofibers was made by depositing well-controlled Fe_2O_3 nanoparticles using sputter coating. The SEM revealed that the diameters of composite nanofiber decreased with the loadings of OMT. The EDX analysis confirmed the existence of OMT and nano- Fe_2O_3 in the nanofiber. The SEM and AFM results indicated the nano- Fe_2O_3 well coated on the surface of homogeneous and cylindrical nanofibers. The TGA results revealed the increased charred residue improved thermal stability properties of the composite nanofiber, due to the superior insulator, mass-transport and physical protective barriers of silicate clay layers and catalysis effects of Fe_2O_3 .

Acknowledgements

The work was financially supported by the Research Fund for the Doctoral Program of Higher Education of China (No. 200802951011), the Natural Science Initial Research Fund of Jiangnan University (No. 2008LYY002) and the Program for New Century Excellent Talents in University (No. NCET-06-0485).

References:

- [1]Giannelis EP, *Applied Organometallic Chemistry* 12 (1998) 675–680.
- [2]Cho JW, Paul DR, *Polym* 42 (2001) 1083–1094.
- [3]Usuki A, Kojima Y, Kawasumi M, Okada A, Kurauchi T, Kamigatio O, *J Mater Res* 8 (1993) 1179–1184.
- [4]Vaia RA, Ishii H, Giannelis EP, *Chem Mater* 5 (1993) 1694–1696.
- [5]Fong H, Liu WD, Wang CS, Vaia RA, *Polym* 43 (2002) 775-780.
- [6]Kim GM, Michler GH, Ania F, Balta Calleja FJ, *Polym* 48(2007)4814-4823.
- [7]Li L, Bellan LM, Craighead HG, Frey MW, *Polym* 47(2006)6208-6217.
- [8]Wang M, Hsieh AJ, Rutledge GC, *Polym* 46 (2005) 3407–3418.
- [9]Laachachi A, Leroy E, Cochez M, Ferriol M, Lopez-Cuesta JM, *Polym Degrad Stab* 89 (2005) 344-352.
- [10]Laachachi A, Cochez M, Ferriol M, Lopez-Cuesta JM, Leroy E, *Mater Lett* 59 (2005) 36-39.
- [11]Laachachi A, Cochez M, Leroy E, Gaudon P, Ferriol M, Lopez-Cuesta JM, *Polym Advan Technol* 17 (2006) 327-334.
- [12]Zong XH, Kim K, Fang DF, Ran SF, Hsiao BS, Chu B, *Polym* 43 (2002) 4403-4412.
- [13]Son WK, Youk JH, Lee TS, Park WH, *Polym* 45 (2004) 2959-2966.
- [14]Liu J, Hu Y, Wang SF, Song L, Chen ZY, Fan WC, *Colloid Polym Sci* 282 (2004) 291-294.
- [15]Allen NS, Harrison MJ, Ledward M, Fellows GW, *Polym Degrad Stab* 23 (1989) 165-174.
- [16]Gilman JW, Jackson CL, Morgan AB, Harris R, Manias E, Giannelis EP, *Chem Mater* 12 (2000) 1866-1873.
- [17]Zhu J, Wilkie CA, *Chem Mater* 13 (2001) 4649-4654.